Macromolecules **2007,** *40,* 4199−4210

2D NMR Studies of Poly(ethylene-*co*-vinyl acetate-*co*-carbon monoxide)

Deepa M. Savant,[†] D. Venkat Reddy,[†] Elizabeth F. McCord,[‡] and Peter L. Rinaldi*,[†]

Department of Chemistry, The University of Akron, Akron, Ohio 44325-3601, and duPont Experimental Station, Bldg 328, Rm 133, Route 141 and Powder Mill Rd, Wilmington, Delaware 19880-328

Received February 6, 2007; Revised Manuscript Received March 21, 2007

ABSTRACT: A series of poly(ethylene-*co*-vinyl acetate-*co*-carbon monoxide) terpolymer samples with varying monomer compositions were studied using a variety of one- and two-dimensional nuclear magnetic resonance (NMR) techniques at 750 MHz. Samples were characterized in deuterated 1,4-dichlocrobenzene-d_4 at high temperature (120 °C) to overcome the signal loss and broadening due to T_2 relaxation. Identification of major triads formed due to the addition of the three monomers in different permutations was facilitated by the use of different 2D techniques such as gradient assisted heteronuclear single-quantum correlation (gHSQC), gradient selected heteronuclear multiple-bond correlation (gHMBC), and gradient assisted HSQC-TOCSY. Detection of unusual structures formed due to the addition of carbon monoxide to vinyl acetate or structures due to the inversion of vinyl acetate was also possible. Because of improved dispersion the study was not restricted to the triad level, but in some cases pentads could also be identified. Distinct resonances of chain ends and short-chain branches were also observed.

Introduction

The study of copolymers from ethylene and vinyl acetate (E−V) or from ethylene and carbon monoxide (E−C) has been described in the past several years.[1−6] This is due to the commercial significance of these polymers in diverse fields. This paper reports 2D NMR studies to elucidate the structures present in poly(ethylene-*co*-vinyl acetate-*co*-carbon monoxide) (polyEVC) and to assign its ^{1}H and ^{13}C NMR resonances.

Addition of different comonomers to polyethylene is done to improve polymer properties, such as strength, flexibility, melting point, and resistance to environmental degradation. PolyEVC[7] terpolymers are often compounded with other plastics to act as tougheners and flexibilizers due to their high tensile strength and tear resistance. The resulting polymer blends find applications in the electrical and automotive industries. They are also used to prepare industrial footwear, athletic shoe soles, roofing membranes, industrial vinyl films, and sheets in construction areas. The structure−property relationship of the polymer is in part dependent upon the monomer sequence distribution which is controlled by the polymerization process, catalysts or initiators used, and the proportions of monomers. Microstructural changes such as tacticity and stereoregularity also have a significant effect on the properties of the polymer. To understand the properties of the polymers and to modify them in a rational way, it is necessary to study the mechanism of polymerization, which is evidenced in the microstructures of the polymers prepared.

NMR spectroscopy has been decisively established as one of the most powerful tools for studying organic structures and is an essential technique for the study of polymers. This is due to the fact that the NMR chemical shift is extremely sensitive to monomer and stereosequence effects. The tacticity studies on poly(V) and poly(EV) copolymers by Ibrahim et al.[8] have revealed that the methylene and methine carbon chemical shifts are especially sensitive to their environments. The monomer sequence distribution (MSD) for triad environments was calculated from the resonance intensities of the methylene and methine groups, and these observed intensities were in turn used to confirm peak assignments. Use of the conformational description (RIS model)[9] and the study of model compounds[10] together with 1D NMR have also been employed for the study of E−V and E−C copolymers. Randall[11] studied polyEV at high temperature (120 °C) to identify the resonances of triads and short alkyl chain branches.

During the course of these studies it was also observed that the copolymers displayed highly overlapping patterns, making it difficult to obtain unambiguous resonance assignments and to determine sequence distributions. Use of two-dimensional (2D) NMR to disperse the resonances helps to resolve and assign some of the resonances in these complicated patterns. This has been demonstrated in the past using 2D experiments such as COSY[12] and HSQC-TOCSY[13,14] to study ethylene containing co- and terpolymers, polyV, and polyEV copolymers.

Spectra of terpolymers are much more complex than those of copolymers due to the overlapping resonances obtained from the many permutations for addition of three monomers in sequence along the polymer chain and stereosequence effects. Because of these difficulties, very little work has been done using NMR to characterize the structures of terpolymers.

Nonetheless, partial chemical shift assignments of some polyEV and polyEC copolymers have been reported in the literature, although the study is at low field using 2D NMR techniques. Recently, Wyzgoski et al.[15] have studied poly(ethylene-*co*-butyl acrylate-*co*-carbon monoxide) terpolymers (polyEBC) at high field (750 MHz) using 2D NMR at high temperature (110 °C). A similar analysis of terpolymer is described here. Because of the complex spectra obtained during the study of such terpolymers, resonance assignments are made for monomer and stereosequences at the triad level. 1D ^{1}H, ^{13}C, and 2D gradient assisted heteronuclear single-quantum coherence (gHSQC),[16] heteronuclear multiple bond correlation (gHMBC),[17] and gHSQC-TOCSY[18,19] experiments at 750 MHz

---

* Corresponding author: Tel 330-972-5990, Fax 330-972-5256, e-mail PeterRinaldi@uakron.edu.

[†] The University of Akron.

[‡] duPont Experimental Station.

10.1021/ma070327l CCC: $37.00

Scheme 1. Structures and Nomenclature for Polyethylene and Poly(ethylene-*co*-vinyl acetate-*co*-carbon monoxide)

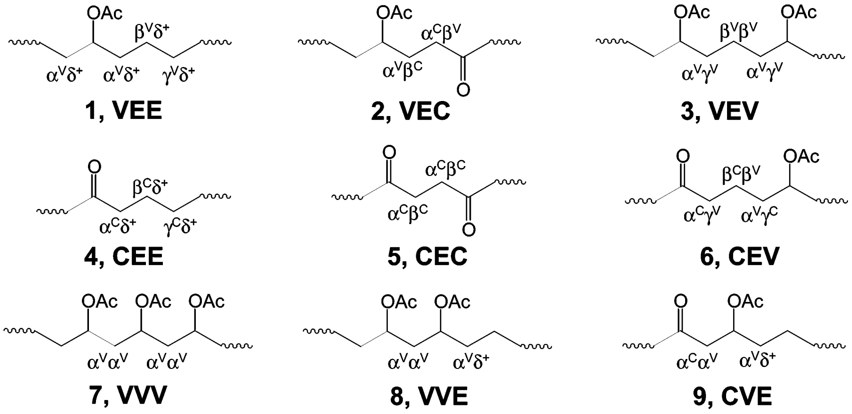

were employed to study four terpolymers having different ethylene/vinyl acetate/carbon monoxide ratios. Elevated temperatures (120 °C) were used to increase the mobility of the samples and thus to lessen the T_2 relaxation effects.

Experimental Section

Preparation of Polymer Samples for NMR Analysis. Four samples of polyEVC—A, B, C, and D—were synthesized at E. I. DuPont de Nemours and Co. by free radical polymerization using ethylene obtained from Sun, carbon monoxide from Messer/MG and vinyl acetate from Celanese. The reaction was initiated via thermal decomposition of organic peroxides. Samples were produces with a flow-through stirred autoclave pilot-plant reactor using high-temperature (150−300 °C) and pressure (15−40 kpsi) reaction conditions. The polymer samples produced were degassed in a polymer separator, fed to a melt pump, and strand cut when feasible. The monomer compositions were determined by 1D ^{13}C NMR. All samples were dissolved in a 1,4-dichlorobenzene-d_4 to produce ca. 8.5% (w/v) polymer solutions. The samples were heated to 120 °C and rotated at 20 rpm in a Kugelrohr oven for 3−5 h to homogenize the solutions. Hexamethyldisiloxane (HMDS) was added in trace quantity to serve as an internal chemical shift reference in both the 1D and 2D NMR spectra ($\delta_H = 0.09$ ppm, $\delta_C = 2.03$ ppm).

Complete details regarding the collection of all NMR data are provided in the Supporting Information.

Results and Discussion

Nomenclature and Structures. The nomenclature used for assigning the carbons in poly(ethylene-*co*-vinyl acetate-*co*-carbon monoxide) is based on the nomenclature used by Randall[11] to describe ethylene/olefin copolymers and modified to account for additional structures formed in ethylene/carbon monoxide/acrylate terpolymers.[15] For completeness, the nomenclature is briefly described here in the context of the structures present in polyEVC.

The carbons along the backbone containing short-chain hydrocarbon branches (Scheme 1) are defined by a pair of Greek letters to indicate the distances, in both directions, to a branch point or a substitution. In addition to the two Greek letters, a superscript “V” or “C” is used to indicate a branch formed from vinyl acetate or carbon monoxide units, respectively. If the in-chain methylene is longer than a certain number of bonds from the branch site, it is indicated by superscripted “+”. The in-chain methine carbons are indicated by “CH” with a subscript indicating the triad structure in which it is centered. For example, in a VEE triad (**1** in Scheme 1) the carbon next to the methine carbon with an acetate branch is designated as α^V; the successive carbons are designated β^V and γ^V. The continuation of the methylene carbon chain in the opposite direction is designated by the second Greek letter, δ^+, indicating that the branch to the right along polymer backbone is in the δ position or further along the polymer chain. Similarly, in a CEV triad (**6**), the carbon adjacent to carbonyl group is designated as $\alpha^C\gamma^V$ since it is α to the C═O branch and it is the third carbon from the methine carbon branch point of a vinyl acetate unit. The next carbon to the right is two bonds away from branches in both the directions along the backbone; it is the second carbon from the carbonyl carbon of a C unit and the second carbon from the methine carbon of a V unit; hence it is designated by $\beta^V\beta^C$. The same system was applied to label groups in all the other triads relevant to the discussion in this paper (Scheme 1).

Table 1 shows the different permutations of triad structures possible in polyEVC. The likelihood of C adding to a growing polymer chain containing terminal C units is low;[20] therefore, structures containing CC dyads are unlikely. At the field strengths used for contemporary NMR studies, the resonances are sensitive to pentad (and even heptad) structures. There can be as many as nine permutations of pentad monomer sequences for each triad structure in Table 1, so that potentially the polymer is a mixture of over 100 structure fragments.

The polymer might also contain short-chain branching structures which are formed by intramolecular H-abstraction and rearrangements that occur during the polymerization process. McCord et al.[21] have extensively studied the formation of short-chain branching in ethylene homopolymer and a variety of ethylene copolymers. Short-chain branches are formed by “backbiting” reactions in which the growing radical chain end curls back to form an intermediate six- or seven-membered ring, transferring the chain end radical back to the main chain by abstracting a hydrogen atom (intramolecular chain transfer). The mechanisms and the nomenclature used by McCord et al. to define the possible short-chain branches have been used to describe the short chains in this study.

1D NMR Spectra. Regions from the ^{13}C NMR spectra (peak-free regions omitted) of the four samples of polyEVC (A, B, C, and D) are shown in Figure 1. The spectra show characteristic features due to their different compositions. As all the different possible peaks are observed in sample A, because of the moderate proportions of all the monomers, it was used as a benchmark to compare the peak intensities in the spectra from the rest of the samples studied. The spectrum of sample B, with highest content of ethylene, shows the most intense peak at 30.00 ppm due to $\delta^+\delta^+$ carbons. Sample C, with highest carbon monoxide content, shows an increase in the intensities of the peaks near $\delta_C = 42$ and 24 ppm due to the α^C and β^C methylene carbons of CEE triads. There is also an increase in the intensity of the $\alpha^C\beta^C$ peak near 36 ppm due to 1,4-dione of CEC structures. The ^{13}C spectrum of sample D, with highest content

Table 1. Possible Triad Sequences for PolyEVC[a]

E-centered	V-centered	C-centered
EEE	EVE	ECE
EEV	EVC	ECC
EEC	EVV(2)	VCE
VEE	CVV(2)	ECV
VEV(2)	CVE	CCV
CEC	VVE(2)	VCV
VEC	VVV(4)	VCC
CEV	VVC(2)	CCE
	CVC	CCC

[a] E = ethylene, V = vinyl acetate, and C = carbon monoxide. The number in the parentheses indicates the number of triad stereosequences when more than one is possible.

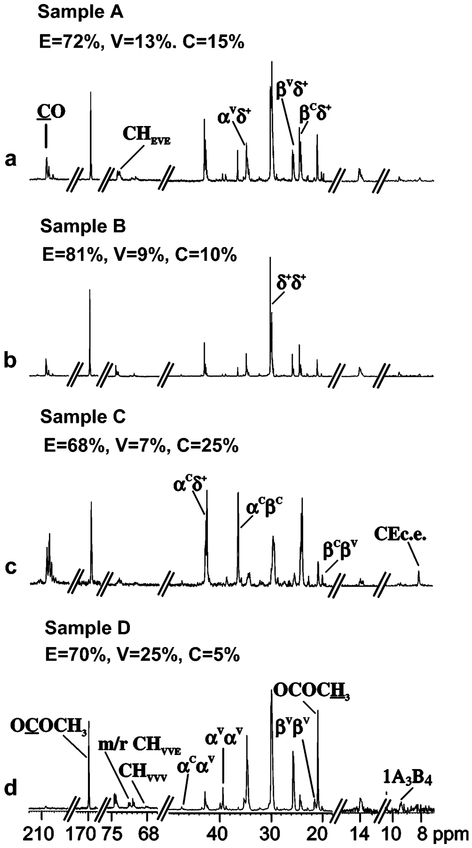

Figure 1. 188.6 MHz ^{13}C NMR spectra of poly(ethylene-*co*-vinyl acetate-*co*-carbon monoxide) samples having varied monomer compositions: (a) sample A ($E = 75\%$, $V = 12\%$, $C = 13\%$); (b) sample B ($E = 81\%$, $V = 9\%$, $C = 10\%$); (c) sample C ($E = 65\%$, $V = 10\%$, $C = 25\%$); (d) sample D ($E = 69\%$, $V = 26\%$, $C = 5\%$).

of V units and the lowest content of C units, shows an increase in the intensities of α^V and β^V methylene resonances of VEE/EEV triads near 34 and 25 ppm, while the peaks from C-centered triads are small compared to the corresponding peaks in the spectra of samples A and C. As the V content in the polymer increases, the $\alpha^V\alpha^V$ methylene carbon peaks due to the less probable triads such as VVV and VVX/XVV are clearly observed in the spectrum near 39 ppm. The methine carbon region also shows many additional resonances from various monomer and stereosequences of -VVX- and -VVV-centered pentads.

The influence of varying the V and C content is also clearly seen in an expansion of the carbonyl region from the ^{13}C spectrum. Sample D shows an increase in the intensities of the resonances from ester carbonyl carbons (~169.7 ppm) compared to the corresponding regions of the spectra from samples A and C. It can also be seen that the intensity of this broad peak is similar to that of the resonance near 20 ppm from the acetate methyl carbon. Because of high content of carbon monoxide units in sample C, the ketone carbonyl intensities are greatly increased.

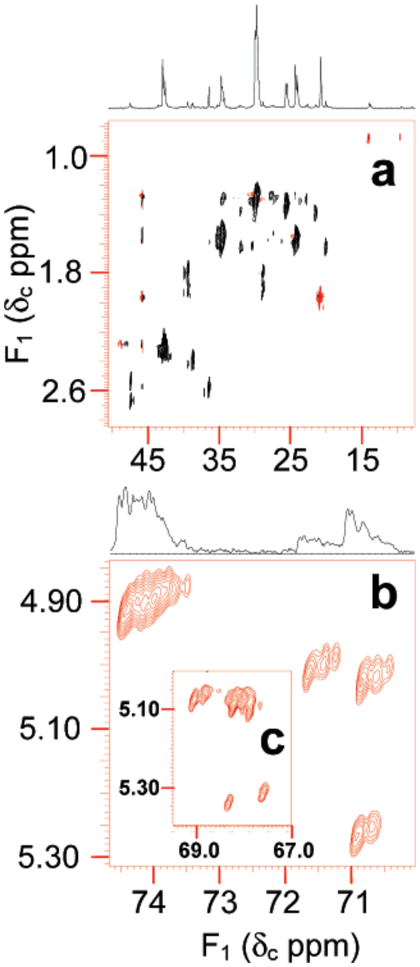

Figure 2. Selected regions from the 2D HSQC NMR spectra of sample A (a) methyl and methylene region and (b) methine carbon region and (c) sample D XVVVX and XCVVX methine carbon region.

The resonances in 1D ^{1}H NMR spectra of polyEVC samples A, B, C, and D also show characteristic changes due to different compositions of E, V, and C in the polymers (figure and detailed explanation provided in the Supporting Information). The resonances which were prominently observed were from chain-end methyl and $-OC(O)CH_3$ protons, $\delta\delta^+$, $\alpha^V\delta^+$, $\alpha^C\delta^+$, and $\alpha^C\beta^C$ methylene protons, and three groups of resonances near $\delta_H = 5$ ppm due to methine protons from various V-centered triads. The downfield region of the ^{1}H spectrum shows two unusual resonances at 6.07 and 6.71 ppm. These are speculated to be from an $\alpha-\beta$ unsaturated ketone unit.

Though the methylene and methine resonances are well separated from each other, the extensive overlap and complexity of the resonance patterns within each group of peaks makes it impossible to do much more than these general resonance assignments using the 1D ^{13}C NMR data. For the complete resonance assignments, experiments like 2D gHSQC, HMBC, and HSQC-TOCSY are useful. They not only give atomic connectivity information but also disperse the spectrum into a second dimension so that overlapping resonances in the 1D spectra can be resolved and assigned unambiguously.

Table 2. Resonance Assignments of Poly(ethylene-*co*-vinyl acetate-*co*-carbon monoxide)

					copolymers					
	assignment		previous works[a]		A		C		D	
region	carbon	polymer sequence	Randall[b] $\delta^{13}C$	Wu[c] $\delta^{13}C$	$\delta^{13}C$[d]	$\delta^{1}H$[e]	$\delta^{13}C$	$\delta^{1}H$	$\delta^{13}C$	$\delta^{1}H$
A	1S	CE			8.04	1.02	7.96	1.00		
	$1A_3B_4$	A_3B_4			9.53	0.87	9.32	0.87	9.49	0.86
	$1B_4$	B4	14.07				14.05	0.89		
	$1B_4$	VEE	14.02		14.03	0.88			14.03	0.88
	$1B_4$				13.95	0.87	13.95	0.87	13.97	0.86
					13.93	0.90				
	$1B_4$	CEE			13.82	0.88	13.82	0.87		
							13.76, 13.79	0.85,0.90		
B	$\beta^{C}\beta^{V}$	CEV			20.01	1.62	19.92	1.62	19.99	1.61
	OCO*C*H$_3$		20.85	21.10	20.84	1.96	20.78	1.96	20.78	1.95
	$\beta^{V}\beta^{V}$	VEV	21.4−21.6	21.10	21.42	1.39			21.39	1.38
	$\beta^{C}\delta^{+}$	CEE		23.80	24.31	1.57	24.25	1.56	24.29	1.56
					24.10	1.55	24.06	1.55	24.10	1.55
	$\beta^{C}\gamma^{C}$	CEEC			23.94	1.55	23.87	1.55	23.92	1.54
					23.73	1.55				
	$\beta^{V}\delta^{+}$	VEE	25.68	25.40	25.65	1.33			25.66	1.32
	$\beta^{V}\gamma^{C}$	V*E*EC			25.47	1.33			25.48	1.32
					25.31	1.33	25.38	1.32	25.31	1.31
C	$\alpha^{V}\beta^{C}$	EV*E*CE			28.80	1.79,1.90			28.78	1.77, 1.89
		VV*E*CE			28.69	1.79,1.89	28.71	1.79,1.90		
	$\gamma^{C}\delta^{+}$	CE*E*EE			29.71	1.27				
	$\delta^{+}\delta^{+}$	EEE			29.95	1.29	29.57	1.26	29.82	1.26
							31.59	1.38, 1.59		
		?			31.98	1.38, 1.63	31.81	1.39, 1.61		
	$\alpha^{V}\delta^{+}$	VEE			34.67	1.55, 1.31			34.65	1.55, 1.30
	$\alpha^{V}\gamma^{C}$	CEVXX			34.21	1.54?				
	$\alpha^{V}\delta^{+}$	VVE			35.24	1.53, 1.60			35.22	1.53, 157
	2S	CE					35.76	2.27		
D	$\alpha^{C}\beta^{C}$	CEC		37.30	36.37	2.57	36.36	2.58	36.36	2.55
	$\alpha^{C}\beta^{V}$	VEC			38.72	2.37	38.62	2.38	38.70	2.35
	$\alpha^{V}\alpha^{V}$	VVE	39.26	39.40	39.34	1.78, 1.91			39.33	1.76, 1.91
	$\alpha^{V}\alpha^{V}$	VVV	39.54	38.80	39.86	1.81, 1.93			39.85	1.80, 1.93
	$\alpha^{C}\delta^{+}$	CEE		42.50	42.85	2.29	42.82	2.29	42.84	2.27
	$\alpha^{C}\gamma^{V}$	CEV			42.38	2.32			42.35	2.31
	$\alpha^{C}\alpha^{V}$ (m)	CVE			47.38	2.52, 2.66	47.29	2.53, 2.67	47.35	2.50, 2.64
	$\alpha^{C}\alpha^{V}$ (r)	CVE			47.02	2.67			47.01	2.65
	$\alpha^{V}\alpha^{C}$ (m)	XCVVX							68.31	5.34
	$\alpha^{V}\alpha^{C}$ (r)								68.22	5.09
E	CH	V*V*V	67−69	67.5, 68.3	68.28	5.11			67.59	5.31
					68.22	5.09			67.99	5.07
									67.88	5.10
									69.03	5.07
									68.83	5.07
		C*V*E			70.90	5.27			70.90	5.26
					70.68	5.25			70.65	5.25
		V*V*E (r)	70.91		70.84	5.03			70.79	5.01
					70.62	5.02			70.55	5.00
					70.44	5.01			70.35	4.99
		V*V*E (m)	71.68	70.1, 70.8	71.64	5.02			71.60	5.00
					71.41	5.00			71.36	4.99
					71.25	4.99			71.15	4.97
		EEVEE	74.45	74.00	74.46	4.93			74.38	4.90
		XE*V*EV			74.15	4.91	74.10	4.89	74.10	4.89
		XE*V*EC			74.00	4.88	73.78	4.89	73.86	4.88
	O*CO*CH$_3$	XEVEX			169.70				169.71	
		XVVEX			169.59				169.56	
		XCVEX			169.40				169.41	
	CO	ECE			208.68				208.70	
		VECEX			207.93					
		CECEV			207.62				207.58	
		ECV			205.95				205.95	

[a] Literature work on EV polymers. [b] Randall, J. C. *J. Macromol. Sci., Rev. Macromol. Chem. Phys.* **1989**, *C29*, 201. [c] Wu, T. K.; Ovenall, D. W.; Reddy, G. S. *J. Polym. Sci., Polym. Phys. Ed.* **1974**, *12*, 901. [d] Digital resolution f_1 = 1.1 Hz/pt. [e] Digital resolution f_2 = 0.6 Hz/pt.

2D NMR of PolyEVC. The HSQC spectrum exhibits correlations between the resonances of ^{1}H and ^{13}C atoms having one-bond scalar couplings ($^{1}J_{CH}$), providing information about connectivity between directly bound ^{1}H and ^{13}C atoms. These correlations are labeled a, b, c, etc., in the spectra. The HSQC spectrum helps to separate the methylenes from the methyl and methine correlations by virtue of the relative signs of the cross-peaks, in place

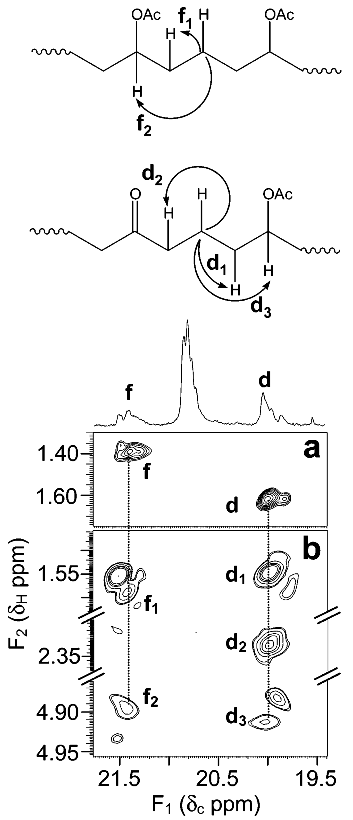

Figure 3. Selected regions from the 2D HSQC (top) and HMBC (bottom) NMR spectra of sample A showing $\beta^V\beta^V$ and $\beta^C\beta^V$ cross-peaks of VEV and CEV triads.

of the 1D DEPT experiment normally used for this purpose.

Figure 2 shows the methyl/methylene (a) and methine (b) regions, from HSQC spectra of sample A. From the spectra it can be observed that the methyl, methylene, and methine resonances are well separated from each other, thus avoiding any phase distortions or cancellation due to the overlap of positive methine and methyl (red) and inverted methylene (black) cross-peaks. The peaks in the HSQC spectrum can be related to multiple-bond correlations in two HMBC spectra obtained using delays optimized for 10 and 5 Hz couplings, respectively (multiple bond delay set to $\tau_{mb} = 1/2^nJ_{CH} = 0.05$ and 0.10). This was done to optimize detection of cross-peaks from two- and three-bonds $^1H-^{13}C$ couplings. These multiple-bond correlations are labeled a_n, b_n, c_n, etc., where the letter designates a specific ^{13}C chemical shift corresponding to the HSQC cross-peak and the numerical subscript n is used to number each of the multiple HMBC correlations at this ^{13}C chemical shift. For example, cross-peak a in the HSQC spectrum can be related to several HMBC cross-peaks (a_1, a_2, a_3, etc.) at the same ^{13}C chemical shift. To confirm the connectivity, a 2D-HSQC-TOCSY experiment was also employed. It gives connectivity between the resonances of ^{13}C atoms and the resonances of all the protons which are part of the spin system of the ^1H atom bound to it. The experiment becomes a very useful tool as it provides the heteronuclear and homonuclear correlations in a single 2D experiment and sometimes reveals correlations not observed in the HMBC spectrum due to cancellations from overlapping antiphase multiplet components in the latter experiment.[22] In the HSQC-TOCSY spectrum, both one-bond and multiple-bond C−H correlations are found. These are designated with the same labels as those used for the corresponding cross-peaks in the HSQC and HMBC spectra. The most intense cross-peak observed in the HSQC spectrum near $\delta_C = 30$ ppm and $\delta_H = 1.29$ ppm is due to the $\gamma\delta^+$ and $\delta^+\delta^+$ protons and carbons from various triads. Resonance assignments from these various experiments employed are summarized in Table 2.

E-Centered Triads. Figure 3 shows the region from the HSQC spectrum of sample A, containing the $\beta^V\beta^V$ and $\beta^V\beta^C$ cross-peaks from VEV and CEV triads, respectively, and the corresponding region from HMBC spectrum showing the multiple-bond correlations to resonances of neighboring ^1H atoms. The $\beta^V\beta^V$ (cross-peaks f) from VEV triads is observed at $\delta_C = 21.42$ ppm and $\delta_H = 1.39$ ppm. This carbon resonance shows a two bond correlations to the $\alpha^V\gamma^V$ ^1H resonance at $\delta_H = 1.59$ ppm (cross-peak f_1) and a long-range correlation to a methine proton at $\delta_H = 4.90$ ppm (cross-peak f_2). The presence of carbonyl carbon in γ-position of a CEV triad instead of an acetate group in a VEV triad shifts the methylene carbon resonance upfield while the protons are shifted downfield. The $\beta^C\beta^V$ resonance of CEV triads is thus observed at $\delta_C = 20.01$ ppm and $\delta_H = 1.62$ ppm (cross-peak d). It shows correlation to two methylene protons two bonds away at $\delta_H = 1.55$ ppm (cross-peak d_1) and $\delta_H = 2.32$ ppm (cross-peak d_2) due to the $\alpha^V\gamma^C$ and $\alpha^C\gamma^V$ groups, respectively, and a three-bond correlation to the CH_{CEVXX} methine proton at $\delta_H = 4.91$ ppm (cross-peak d_3).

The addition of vinyl acetate in an opposite manner may take place during the polymerization process; this can be observed in the CE $\bar{V}$ triads (indistinguishable from VEC triads). Figure 4 shows the regions from HSQC-TOCSY spectrum containing VEC triad cross-peaks. The HSQC-TOCSY spectrum shows correlations to protons in a spin-coupled system in addition to one-bond carbon−proton correlations. The $\alpha^V\beta^C$ resonance (cross-peak i) due to the one-bond carbon−proton correlation is observed at $\delta_C = 28.80$ ppm and $\delta_H = 1.79$, 1.90 ppm. Correlations to $\alpha^C\beta^V$ (cross-peak i_1) and CH_{XXVEC} (cross-peak i_2) proton resonances are observed at $\delta_H = 2.37$ ppm and $\delta_H = 4.91$ ppm, respectively. Similarly, a one-bond carbon−proton correlation to the $\alpha^C\beta^V$ proton resonance (cross-peak m) is obtained at $\delta_C = 38.72$ ppm and $\delta_H = 2.37$ ppm while a clear correlation to the nonequivalent $\alpha^V\beta^C$ protons (cross-peaks m_1) is seen at $\delta_H = 1.79$ and 1.90 ppm; correlation to CH_{XXVEC} proton (cross-peak m_2) is seen at $\delta_H = 4.91$ ppm.

A group of resonances at around $\delta_C = 25$ ppm in HSQC spectrum are due to β^V methylene correlations in VEE/EEV triads (Figure 1). The fine structure observed is due to the effect of neighboring monomer units (E, V, or C). The $\beta^V\delta^+$ of VEEE tetrads is observed at $\delta_C = 25.65$ ppm and $\delta_H = 1.33$ ppm, and that of $\beta^V\gamma^C$ of VEEC tetrad is observed at $\delta_C = 25.47$ ppm and $\delta_H = 1.33$ ppm in the HSQC spectrum (see Supporting Information).

All the $\alpha^V\delta^+$ and $\alpha^V\gamma^C$ resonances are observed near $\delta_C = 34.4$ ppm and $\delta_H = 1.60$ ppm in the plot of the regions from the HSQC-TOCSY spectrum shown in Figure 5. The HSQC peak pattern is extremely complex due the various $\alpha^V\gamma^X$ resonances in this region. The substitution at the γ position has a very minor effect on the chemical shift of the $\alpha^V\gamma^X$ carbons; hence, the correlations show severe overlap. The most upfield correlation ($\delta_C = 34.20$ ppm and $\delta_H = 1.56$ ppm, cross-peak k′) is due to the $\alpha^V\gamma^C$ methylene groups of CEVX tetrads. This carbon shows correlations to the resonances of three types of neighboring protons: correlation k'_1 to the $\beta^V\beta^C$ proton resonance, correlation k'_2 to the $\alpha^C\gamma^V$ proton resonance, and correlation k'_3 to the CH_{CEVX} proton resonance. The $\alpha^V\delta^+$ signal (cross-peak k″) due to EEVX tetrads is observed at $\delta_C = 34.65$

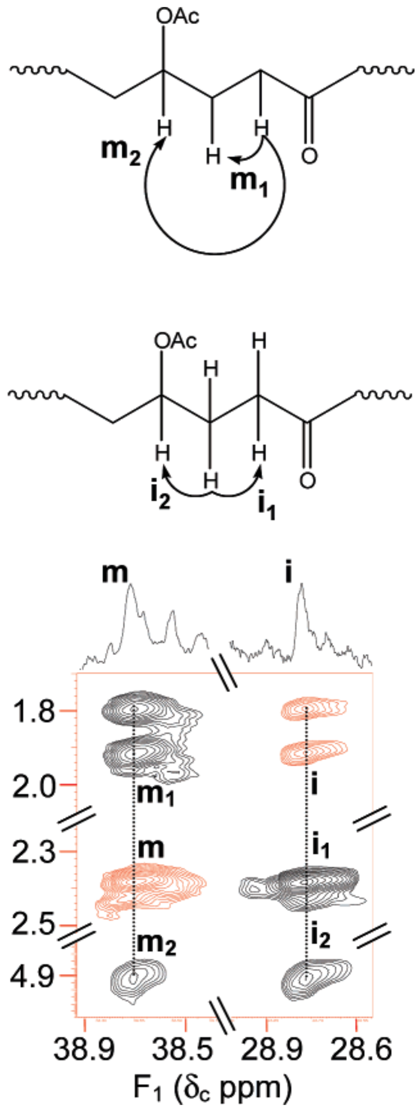

Figure 4. Selected regions from the 2D NMR spectra of sample A showing $\alpha^V\beta^C$ and $\alpha^C\beta^V$ cross-peaks of VEC triad: HSQC-TOCSY 2D NMR spectra.

ppm and $\delta_H = 1.57$ ppm in the HSQC-TOCSY spectrum, and the $\alpha^V\delta^+$ carbon resonance shows correlations to the resonances of neighboring $\beta^V\delta^+$ protons (cross-peak k''_1) and to the methine proton at $\delta_H = 4.94$ ppm (cross-peak k''_2). The most downfield correlation (k''') is observed at $\delta_C = 35.20$ ppm, and $\delta_H = 1.55$ and 1.60 ppm is at the ^{13}C shift of the resonance from the $\alpha^V\delta^+$ methylenes of VVEX tetrads. This carbon resonance shows correlations to the $\beta^V\delta^+$ proton resonance (cross-peak k'''_1) at $\delta_H = 1.34$ ppm and to the CH_{VVE} methine proton resonance at $\delta_H = 5.05$ ppm (cross-peak k'''_2).

The group of resonances observed in the HSQC spectrum at $\delta_C = \sim 24$ ppm are due to β^C of CEE triads and shows fine structure due to different substitutions possible. Two of the resonances, i.e., $\beta^C\delta^+$ in the ECEE tetrads and $\beta^C\gamma^C$ in ECEEC pentad, could be assigned. The resonances were confirmed with the help of HMBC correlations (see Supporting Information).

The group of resonances observed in the extreme downfield region ($\delta_C = \sim 42$ ppm) of the HSQC spectrum is due to α^C carbons and protons of ECEE and ECEV tetrads (Figure 6). The $\alpha^C\delta^+$ resonance of the ECEE tetrad is observed at $\delta_C = 42.85$ ppm and $\delta_H = 2.29$ ppm (cross-peak p') while the $\alpha^C\gamma^V$ carbon resonance from the ECEV tetrad is shifted upfield to $\delta_C = 42.38$ ppm due to γ-gauche effect but the proton resonance is shifted downfield, at $\delta_H = 2.32$ ppm (cross-peak p''''). The $\alpha^C\delta^+$ resonance of ECEE tetrads show correlations to the $\gamma^C\delta^+$ protons at $\delta_H = 1.28$ ppm (cross-peak p'_1) and to $\beta^C\delta^+$ protons at $\delta_H = 1.57$ ppm (cross-peak p'_2). The ECEV tetrad shows correlations to $\beta^C\beta^V$ protons at $\delta_H = 1.62$ ppm (cross-peak p''''_1) and to $\alpha^V\gamma^C$ protons at $\delta_H = 1.57$ ppm (cross-peak p''''_2).

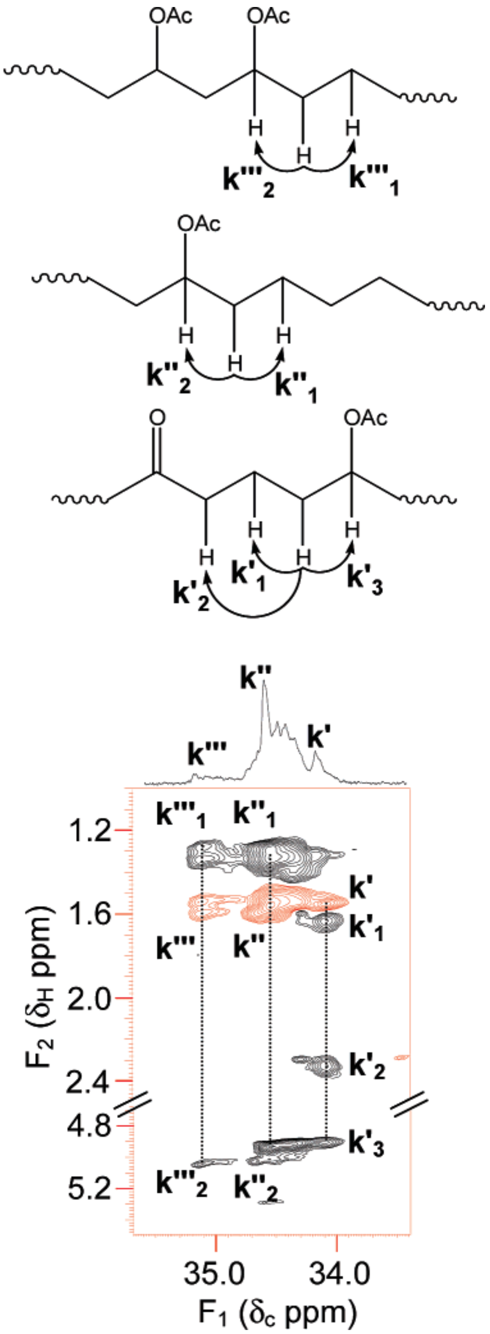

Figure 5. Selected regions from the 2D HSQC-TOCSY NMR spectra of sample A showing $\alpha^V\delta^+$ and $\alpha^V\gamma^C$ cross-peaks.

The CEC triad is very symmetrical and has one type of carbon between two ketone carbonyl carbons, the $\alpha^C\beta^C$ carbon. The $\alpha^C\beta^C$ one-bond C−H correlation is observed at $\delta_C = 36.37$ ppm, and $\delta_H = 2.57$ ppm in HSQC. It shows a correlation in HMBC at the same chemical shift ($\delta_H = 2.57$ ppm) as in HSQC as both the $\alpha^C\beta^C$ carbons and protons are equivalent (see Supporting Information).

V-Centered Triads. Although $\alpha^V\alpha^V$ methylene carbon resonances from XVVE and XVVV tetrads are very close in

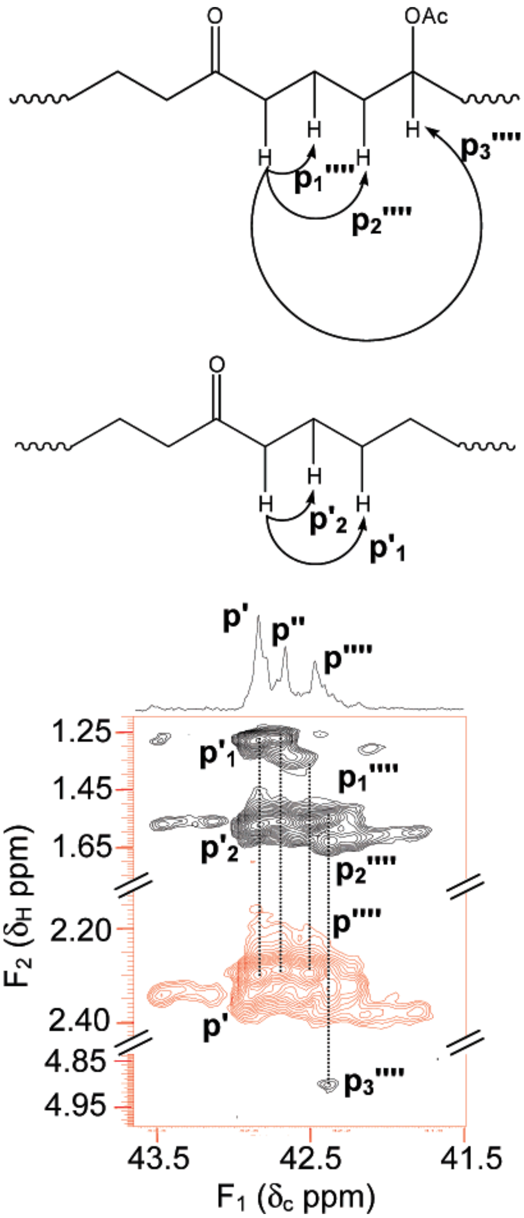

Figure 6. Selected regions from the 2D HSQC-TOCSY NMR spectra of sample A showing α^C cross-peaks of ECE and CEV triads.

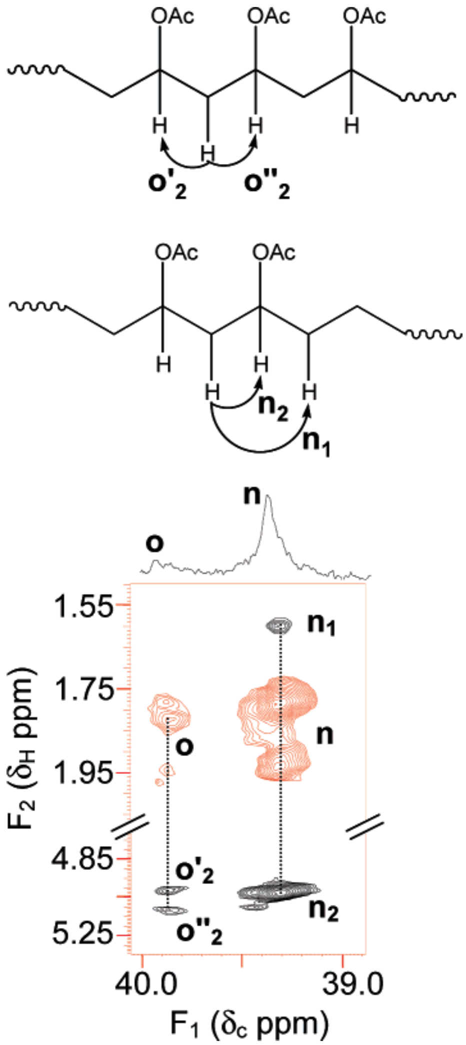

Figure 7. Selected regions from the 2D HSQC-TOCSY NMR spectra of sample A showing $\alpha^V\alpha^V$ cross-peaks of VVE and VVV triads.

the ^{13}C 1D spectrum, 2D experiments help to disperse them into two distinct sets of contour peak patterns as seen in the HSQC-TOSCY spectrum in Figure 7, which provides information about the neighboring groups in XVVE and XVVV tetrads.

The cross-peaks *n* in the HSQC-TOCSY spectrum are due to one-bond correlations between $\alpha^V\alpha^V$ methylene group carbon and proton resonances of EVVE tetrads (δ_C = 39.34 ppm and two nonequivalent proton at δ_H = 1.78 and 1.91 ppm). Correlations are observed to the neighboring methine proton at δ_H = 5.03 ppm (cross-peak n$_2$) and to the $\alpha^V\delta^+$ protons at δ_H = 1.61 ppm (cross-peak n$_1$). A symmetric structure would result in a correlation to one CH proton resonance as observed in the case of the EVVE tetrad, while the $\alpha^V\alpha^V$ methylene in the central VV dyad in a EVVV tetrad shows two resolved one-bond C−H correlation in the HSQC-TOCSY spectrum which was not evident in HMBC. These cross-peaks are due to proton resonances of CH$_{EVV}$ and CH$_{VVV}$ groups on either side (cross-peaks o$_{2'}$ and o$_{2''}$), respectively.

Addition of carbon monoxide to vinyl acetate is expected to occur preferentially to the methylene group of V after an inverse addition to form an *E$\bar{V}$C* triad, which would be indistinguishable from CVE. Addition of C═O to a terminal V methine carbon to form EVC triads would be unexpected on the basis of steric and electronic effects. The resonance observed at ∼47 ppm in ^{13}C 1D spectrum of all four polymers is consistent with the shift of $\alpha^C\alpha^V$ carbons in CV dyads. The intensity of this peak is highest in sample C. Because of the effect of the ketone carbonyl and the methine carbon with an acetate group in the α position, the $\alpha^C\alpha^V$ resonance from the CVE triad is observed in the downfield region (mδ_C = 47.38 ppm, mδ_H = 2.52, 2.66 ppm and rδ_C = 47.02 ppm, rδ_H = 2.67 ppm) of the HSQC spectrum (Figure 8) and shows TOCSY correlations to only the neighboring methine proton at δ_H = 5.28 ppm.

Various CH$_{XVX}$ methine correlations are observed between δ_C = 70−75 ppm and δ_H = 4.80−5.30 ppm (Figure 2b). The cross-peaks due to the XE*V*EX, VE*V*XX, XX*V*EV, CE*V*XX, and XX*V*EC pentads are observed between δ_C = 73−75 ppm and δ_H = 4.85−4.95 ppm. The right half of this region (δ_C = 70−72 ppm) contains correlations from CH$_{VVE/EVV}$. Groups of resonances observed between δ_C = 70.54−71.01 ppm but much further downfield than all the other resonances in the f_2 dimension (δ_H = 5.23−5.30 ppm) are due to CVE or $\bar{V}$CE triads. The HSQC-TOCSY spectrum (Figure 9) gave better connectivity information; hence, it was used to assign the major methine resonances. The most downfield resonance (cross-peak t′, δ_C = 74.46 ppm and δ_H = 4.93 ppm) is due to CH$_{EE\mathit{V}EE}$ and shows

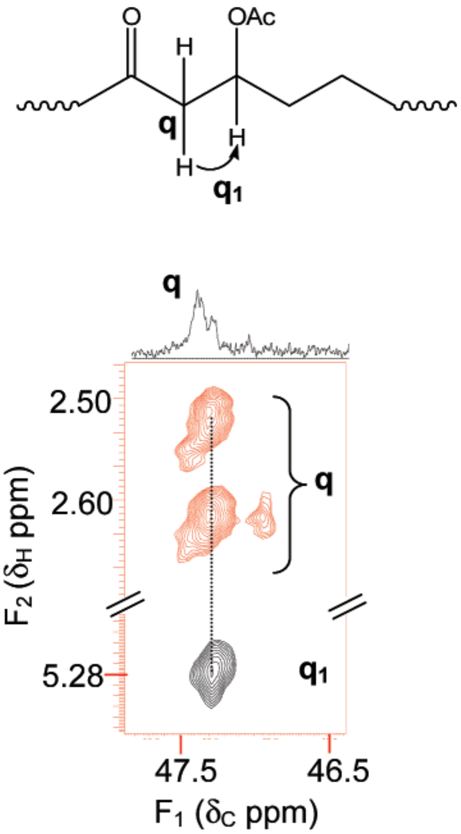

Figure 8. Selected regions from the 2D HSQC-TOCSY NMR spectra of sample C showing $\alpha^C\alpha^V$ cross-peaks of CVE triads.

correlations to $\alpha^V\delta^+$ protons at $\delta_H = 1.56$ ppm (t'_2) and to $\beta^V\delta^+$ protons at $\delta_H = 1.33$ ppm (t'_1). The CH_{VEVEX} resonance is observed at $\delta_C = 74.15$ ppm and $\delta_H = 4.91$ ppm (cross-peak t″). Wu and Ovenall[2,3] observed the methine resonance of EE*V*EV pentads in polyEV at 74.1 ppm. The next upfield resonance is assigned to CH_{XXVEC}, which is observed at $\delta_C = 74.00$ ppm and $\delta_H = 4.91$ ppm (cross-peak t‴) and shows correlations to $\alpha^V\beta^C$ protons at $\delta_H = 1.80$, 1.93 ppm (t'''_3) and to the $\alpha^C\beta^V$ protons at $\delta_H = 2.38$ ppm (t'''_4). Further correlations at $\delta_H = 1.56$ ppm and at $\delta_H = 1.33$ ppm (due to $\alpha^V\delta^+$, t'''_2 and $\beta^V\delta^+$ protons, t'''_1) confirms the presence of an ethylene unit on the other side of “V” in the XX*V*EC pentad.

The methine resonances of V*V*E triads (Figure 9) occur in two groups, the first group containing cross-peaks from *r*-VV dyads (cross-peak r′, $\delta_C = 70.84$ ppm, $\delta_H = 5.04$ ppm) and a second group containing cross-peaks from *m*-VV dyads (cross-peak s, $\delta_C = 71.64$ ppm, $\delta_H = 5.01$ ppm) due to the relative orientations of the acetate branches. At the ^{13}C shift of the *m*-CH_{VVE} in the HSQC-TOCSY cross-peaks are seen to the $\alpha^V\delta^+$ protons at $\delta_H = 1.60$ ppm (cross-peak s_1) and to the nonequivalent $\alpha^V\alpha^V$ protons at $\delta_H = 1.79$ and 1.93 ppm (cross-peaks s_2). Racemic methine carbon resonances are correlated to $\alpha^V\delta^+$ protons at $\delta_H = 1.60$ ppm (cross-peak r'_1) and to only a single proton resonance from equivalent $\alpha^V\alpha^V$ protons at $\delta_H = 1.80$ ppm (cross-peak r'_2).

In CVE triads, because of the presence of the ketone carbonyl group in the β position relative to the CH_{CVE}, the methine proton resonance is downfield (Figure 2b) compared to the corresponding CH_{EVE} and CH_{VVE} resonances. Cross-peaks from these triads (Figure 10) are clearly observed in the HSQC spectrum at $\delta_C = 70.96$ ppm and $\delta_H = 5.27$ ppm (cross-peak r″); correlations to the diastereotopic $\alpha^C\alpha^V$ protons are observed at $\delta_H = 2.53$ and 2.67 ppm (cross-peaks r''_1) in the HMBC spectrum.

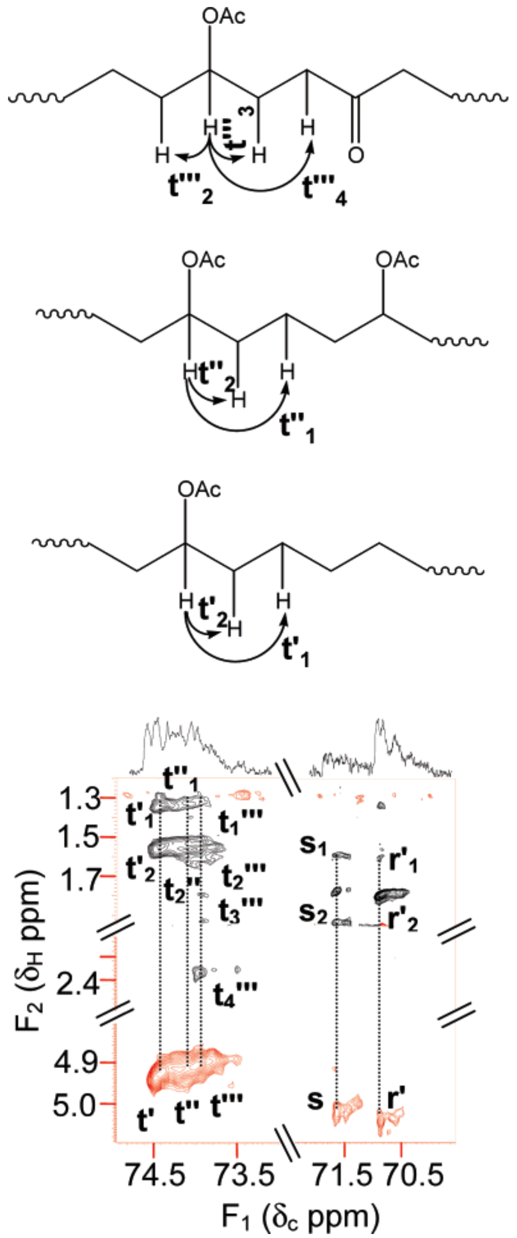

Figure 9. Selected regions from the 2D HSQC-TOCSY NMR spectra of sample A showing methine resonances of EVE, VEC, VEV, and VVE triads.

Examination of the ^{13}C spectrum from sample D in the methine region ($\delta_C = 67.4-69.4$ ppm) shows additional peaks compared to those found in the spectra from the other three samples. These are attributed to the VVV triads which are much more probable in this polymer having high V-content. The HSQC spectrum (Figure 2c) of this sample in the same region shows that the peaks are widely separated into two groups along the proton chemical shift dimension. By analogy with our resuts for EVV and EVC triads, we can assign the peaks at $\delta_C = 68$ ppm and $\delta_H = 5.1$ ppm to VVV and the resonances ($\delta_C = 67.59$ ppm and $\delta_C = 68.31$ ppm) downfield along the proton chemical shift ($\delta_H = 5.31$ ppm and $\delta_H = 5.34$ ppm) to CVV triads. Two peaks are observed due most likely to the stereochemical arrangements (*m* and *r*) of the acetate pendant groups.

Ester Carbonyl Resonances. The ester carbonyl carbons are away from the main chain and hence are not as sensitive to the changes in the monomer structure two or three units down the chain. Nevertheless, they show some sensitivity toward the monomer sequence effects in triads. The HMBC slices show

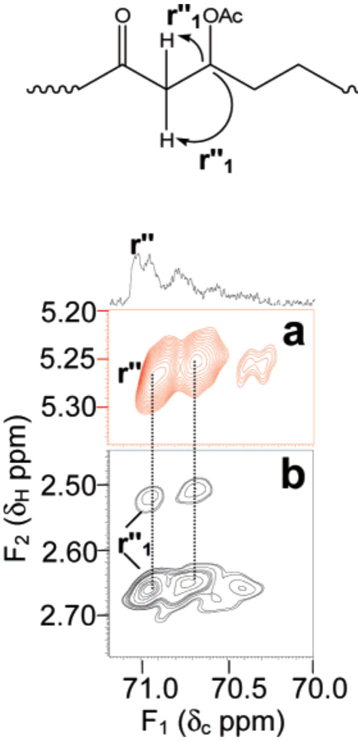

Figure 10. Selected regions from the 2D HSQC (top) and HMBC (bottom) NMR spectra of sample A showing methine resonances of CVE triads.

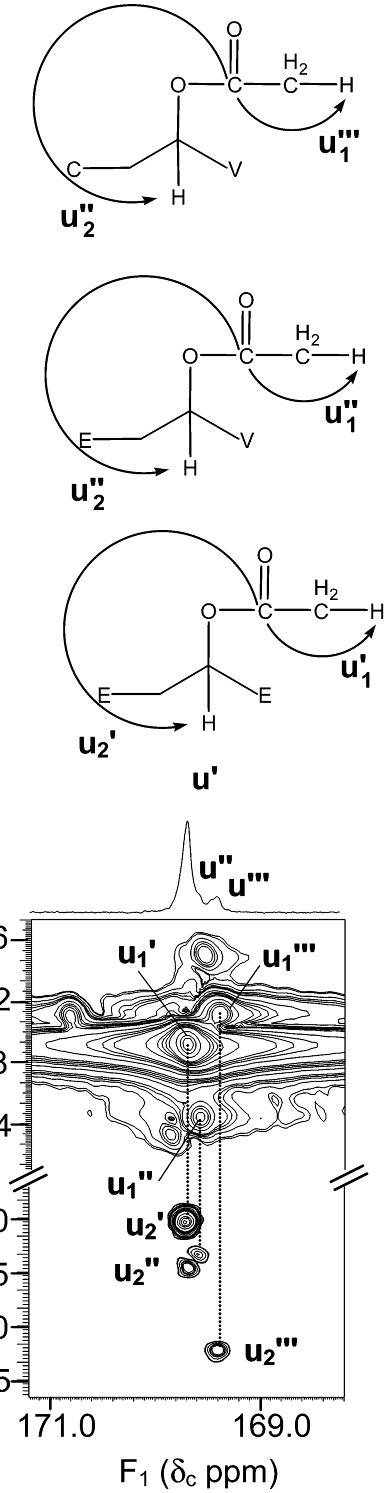

Figure 11. Selected regions from the 2D HMBC NMR spectra of sample A showing ester carbonyl resonances.

correlations between the ester-carbonyl carbon and methyl proton resonances. Very weak correlations can also be observed to the methine protons. Figure 11 shows the correlations of ester carbonyl carbons in various triads to the methyl protons and the corresponding methine protons. The three easily identified ester carbonyl carbon resonances are from XE*V*EX, XE*V*VE, and XC*V*EX pentads. All the XE*V*EX ester carbonyl carbon resonance at $\delta_C = 169.70$ ppm show correlations to the methyl protons at $\delta_H = 1.96$ ppm (cross-peak u'_1) and to the methine proton resonance at $\delta_H = 4.91$ ppm (cross-peak u'_2).

Replacement of an E unit in EVE triads with a V unit to produce E*V*V triads shifts the ester carbonyl carbon resonance upfield ($\delta_C = 169.59$ ppm). Correlations from this carbon resonance are observed with the methyl protons at $\delta_H = 1.93$ ppm (cross-peak u''_1) and methine proton resonance at $\delta_H = 5.00$ ppm (cross-peak u''_2). Replacement of E unit in EVE triads with a C to produce C*V*E triads also shifts the ester carbonyl carbon resonance up field ($\delta_C = 169.40$ ppm), but only slightly. Correlations from this carbon resonance are observed with the methyl protons at $\delta_H = 1.93$ ppm (cross-peak u'''_1) and to the methine proton at $\delta_H = 5.27$ ppm (cross-peak u'''_2).

C-Centered Triads. The ketone carbonyl carbon resonances are observed in three groups, centered near 208 ppm (E*C*E), 207 ppm (VE*C*XX, CE*C*XX), and 206 ppm (XE*C*VX) (Figure 12). The ketone carbonyl carbon at 208.68 ppm is due to ECE triads and shows correlations to the $\alpha^C\delta^+$ and $\beta^C\delta^+$ protons at 2.30 ppm (cross-peak x_2) and 1.58 ppm (cross-peak x_1), respectively. Addition of a V next to an E in ECE triad shifts the ketone carbonyl resonance upfield. Thus, the resonance at 207.93 is due to VE*C*EX pentad, and it shows correlations to $\alpha^C\beta^V$ protons at 2.38 ppm (cross-peak w_3), α^C protons at 2.29 ppm (cross-peak w_2), and $\alpha^V\beta^C$ protons at 1.80 ppm (cross-peak w_1). The resonance at $\delta_C = 207.62$ ppm is observed due to the occurrence of a C and a V next to E in the ECE triad and gives rise to CE*C*EV pentad. The ketone carbonyl shows correlations to $\alpha^C\beta^C$ protons at 2.57 ppm (cross-peak w'_3) and $\alpha^C\gamma^V$ protons at 2.34 ppm (cross-peak w'_2). The highest ketone carbonyl carbon resonance at $\delta_C = 206.00$ ppm (cross-peak v) is due to XE*C*VX pentads. The carbonyl carbon shows correlations to the β^C protons at 1.57 ppm and a set of resolved correlation to the $\alpha^C\alpha^V$ diastereotopic protons at 2.52 ppm and 2.67 ppm (cross-peaks v_2). Correlations to the α^C protons could not be resolved and assigned here as the resonances fall on the tails of the more prominent resonances at ~208 ppm.

Figure 12 (sample A) shows the correlations observed for E*C*V triads at $\delta_C = 205.95$ ppm in the HMBC spectrum. The ketone carbonyl carbon shows correlations to only the two

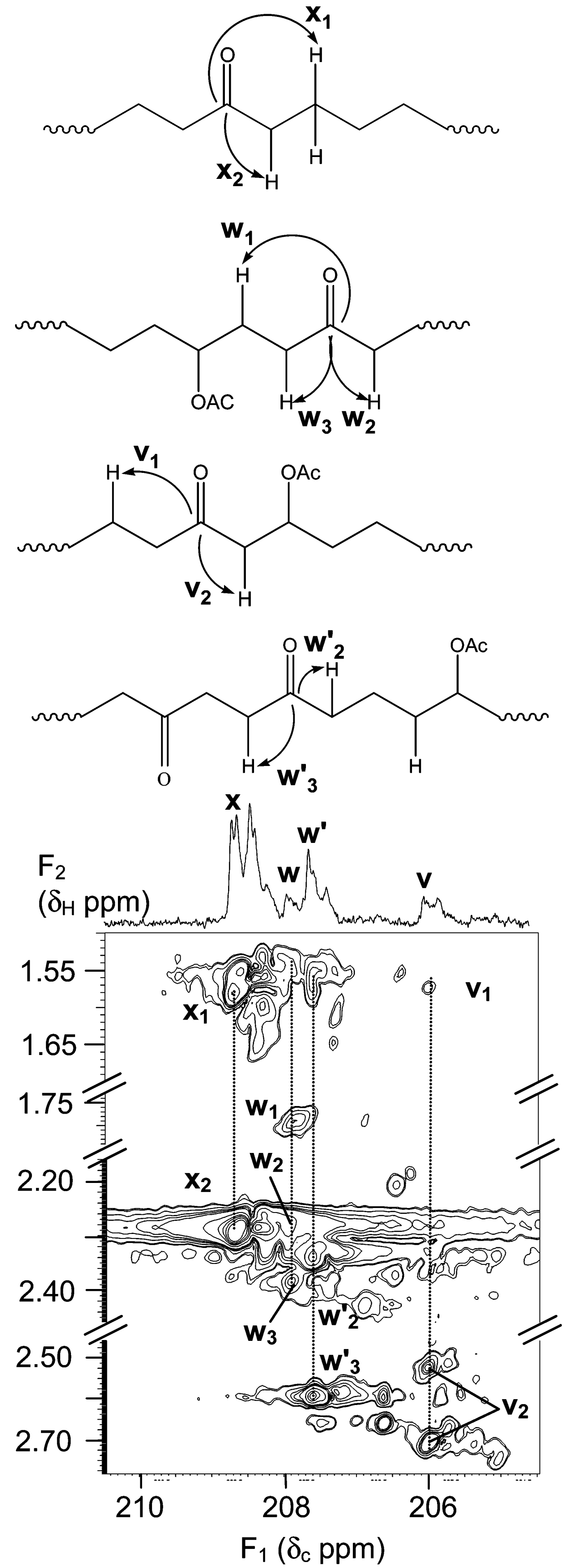

Figure 12. Selected regions from the 2D HMBC NMR spectrum of sample A showing correlations to ketone carbonyl resonances.

diastereotopic protons at $\delta_H = 2.52$ and 2.66 ppm (cross-peak v_1). These correlations are to the two nonequivalent $\alpha^C\alpha^V$ protons. Further correlations were found neither in polymer with high vinyl acetate content (sample D) nor in the polymer with high carbon monoxide content (sample C).

Chain Ends and Short-Chain Branching (SCB). As the polymer is a terpolymer, various chain ends are possible.[23] Additionally, terminal methyl resonances due to short-chain branching (SCB) are also possible. McCord et al.[21] have studied SCB in E/V copolymers and identified the terminal methyl ^{13}C resonance at $\delta_C = \sim 9.5$ ppm to be the A_3B_{4+} structure. Others have studied E/CO copolymers and identified resonances from characteristic CO-containing branches and chain ends.[5,29] All the polymers studied here show three distinct peaks at $\delta_C \sim 8.0$, ~ 9.4, and ~ 13.9 ppm (Figure 13) (*positions slightly different in the spectra of individual samples may be due to the effect of adjacent groups*); the intensities change depending on the relative concentrations of the three monomers in the polymers. Sample C with high carbon monoxide content shows increased intensity of the cross-peak at $\delta_C = 7.97$ ppm and $\delta_H = 1.00$ ppm (cross-peak a) in the HSQC spectrum (Figure 13), and it is assigned to a CE branch end or chain-end methyl group. It shows a correlation in the HMBC at $\delta_C = 35.75$ ppm (cross-peak a_1) to the methylene carbon of the CE ethyl group; no correlation to the carbonyl carbon could be observed in the HMBC spectrum.

Correlations consistent with the $1A_3B_{4+}$ at $\delta_C = 9.49$ ppm and $\delta_H = 0.86$ ppm (Figure 13, cross-peak b) were observed in sample D (Figure 13b). This shows correlations to a $2A_3B_{4+}$ carbon resonance at 27.42 ppm (cross-peak b_1) and a weak correlation to the methine carbon resonance at 75.53 ppm (cross-peak b_2). Although the $1A_3B_{4+}$ peak is evident in the 1D spectra of all the polymers studied, the intensity is very low in sample D with the highest percentage (~55%) of vinyl acetate, while the intensity grows in polymers with the highest percentages of ethylene (samples A and B). This suggests that the high amounts of C in the backbone inhibit the backbiting reaction sterically and/or electronically.

Cross-peaks labeled c, attributed to the various terminal methyls (1s) in straight segments of hydrocarbon chains, are observed near $\delta_C = 13.96$ ppm and $\delta_H = 0.87$ ppm. Correlations to the 2s methylene carbons are seen at $\delta_C = 22.66$ ppm (cross-peak c_1) and to 3s methylene carbon at $\delta_C = 32.29$ ppm (cross-peak in region c_6).

The cross-peak at $\delta_C = 23.4$ ppm is characteristic of a $2B_4$ carbon of a butyl branch. Some of the cross-peaks in the $\delta_C = 26-28$ ppm region might indicate a VEE chain end, and there is likely a peak in the crowded $\delta_C = 22.9$ ppm region for a CEE end. This region is complex and resonances in this region can arise from many different possible structures.

Figure 13c shows the cross-peaks near 13.9 ppm from the HSQC spectrum of sample A. These are due to methyl groups at chain ends or the ends of branched structures of length butyl or higher (1s, B_5^+, B_4, VEEc.e, CEEc.e, etc.). Correlations to various carbons and protons along the chain can be observed in the HMBC spectrum. Correlations to 2s, $2B_5^+$, 2s of VEEc.e, and 2s of CEEc.e can be observed as a cluster of resonances at $\delta_C = \sim 22.7$ ppm (cross-peaks c_1) while correlations to $2B_4$ carbons are observed at $\delta_C = 23.4$ ppm (cross-peaks c_2). The 3s carbons of VEEc.e and CEEc.e are observed at $\delta_C = \sim 26.2$ ppm (cross-peaks c_3), cross-peaks to $3B_4$ carbons occur in the more downfield region ($\delta_C = \sim 29.6$ ppm (cross-peaks c_5), and 2s, $3B_5^+$ were observed furthest downfield at $\delta_C = \sim 32.3$ ppm (cross-peaks c_6). Because of the probability of forming many different chain-end structures, the spectrum shows many overlapping cross-peaks in this region; hence, the resonances in the HMBC spectrum are assigned as a group.

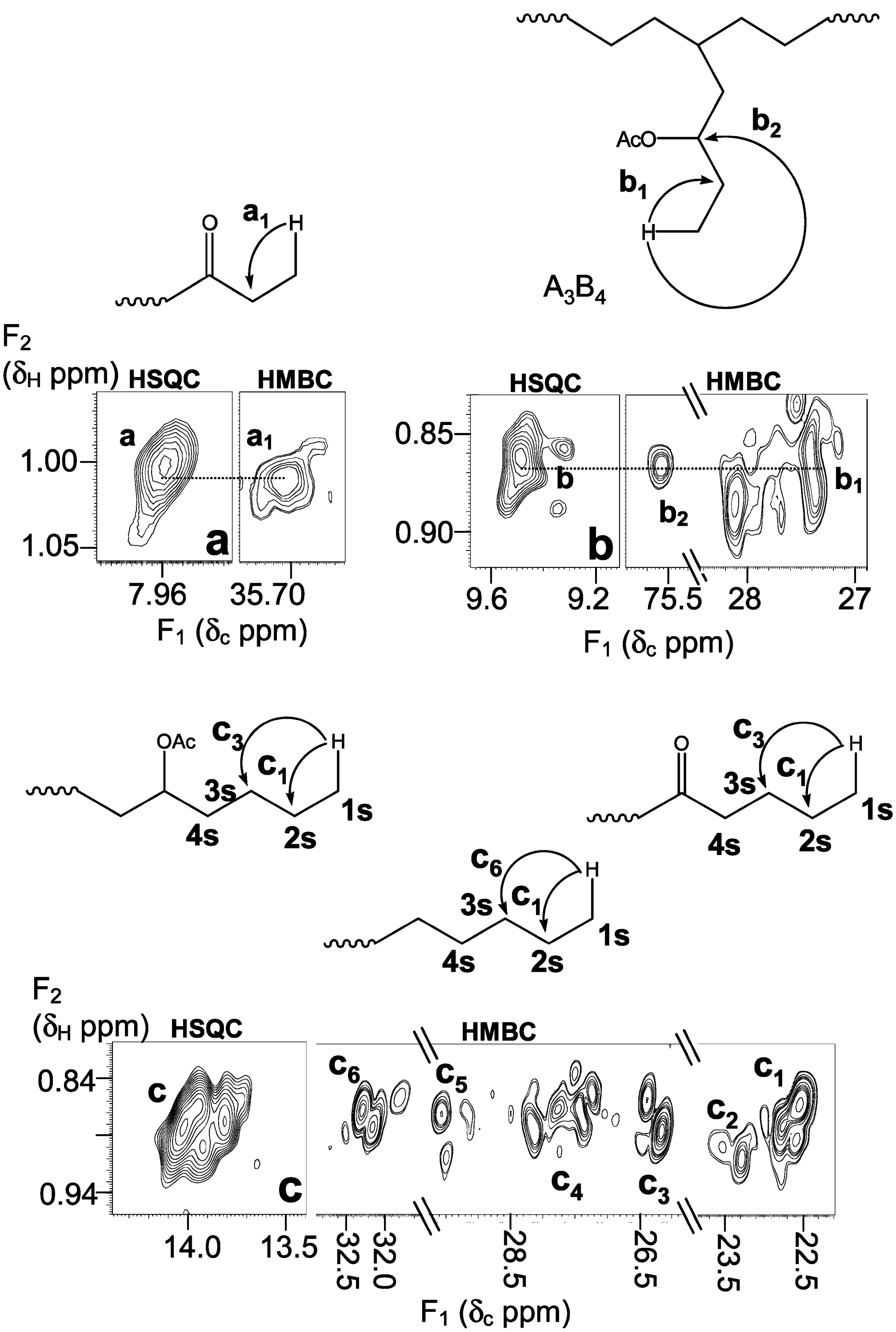

Figure 13. Correlations from chain ends and short chain branches in sample A (bottom, c), sample C (upper left, a), and sample D (upper right, b) in the HSQC and HMBC 2D NMR spectra.

Conclusions

A systematic study of the four poly(ethylene-*co*-vinyl acetate-*co*-carbon monoxide) samples with varying amounts of monomers demonstrates the utility of 2D NMR techniques in characterizing complex polymers. The techniques were useful for unequivocal assignments of resonances from a range of triad monomer sequence structures and for identifying tacticity effects, which was not possible by one-dimensional NMR. gHSQC experiments allowed separation and identification of methyl, methylene, and methine resonances from each other; HSQC-TOCSY proved to be a valuable adjunct to gHMBC, often giving information on two-bond correlations which are not evident in the gHMBC spectra. A few chain ends and short-chain branching structures can also be identified from the 2D NMR experiments. In accordance with the study of EV polymers of McCord et al., no evidence was found for quaternary carbons, indicating that backbiting or chain transfer to the acetate methine does not occur at a detectable level. Although it was possible to assign all the major triads, many resonances could not be assigned due to spectral overlap; hence, work is continuing using 3D NMR with isotopic labeling to selectively study the resonances in congested regions of these spectra.

Acknowledgment. The authors thank the National Science Foundation (DMR-0073346 and DMR-0324964) and E. I. du Pont de Nemours and Co for the support of this work and Kresge Foundation and donors to the Kresge Challenge program at the University of Akron for the funds used to purchase the 750 MHz NMR instrument used. The authors also acknowledge J. Massey and S. Stakleff for their technical assistance in maintaining the NMR facilities used for this work.

Supporting Information Available: Selected plots of 2D spectra and labeled structures that show additional resonance assignments in Table 2, not explicitly discussed in the body of this paper; detailed information on the collection and processing of NMR data. This material is available free of charge via the Internet at http://pubs.acs.org.

References and Notes

(1) Delfini, M.; Segre, A. L.; Conti, F. *Macromolecules* **1973**, *6*, 456.

(2) Wu, T. K.; Ovenall, D. W.; Reddy, G. S. *J. Polym. Sci., Polym. Phys. Ed.* **1974**, *12*, 901.

(3) Wu, T. K.; Ovenall, D. W. *Macromolecules* **1974**, *7*, 776.

(4) Sung, H. N.; Noggle, J. H. *J. Polym. Sci., Polym. Phys. Ed.* **1981**, *19*, 1593.

(5) Bovey, F. A.; Gooden, R.; Schilling, F. C.; Winslow, F. H. *Macromolecules* **1988**, *21*, 938.

(6) de Souza, C. M. G.; Tavares, M. I. B. *Polym. Test.* **1998**, *17*, 533.

(7) http://dupont.com.

(8) Ibrahim, B.; Katritzky, A. R.; Smith, A.; Weiss, D. *J. Chem. Soc., Perkin Trans. 2* **1974**, 1537.

(9) Tart, E.; Wood, G.; Wernsman, D.; Sangwatanaroj, U.; Howe, C.; Zhou, Q.; Zhang, S.; Tonelli, A. E. *Macromolecules* **1993**, *26*, 4283.

(10) Cheng, H. N.; Lee, G. H. *Macromolecules* **1988**, *21*, 3164.

(11) Randall, J. C. *J. Macromol. Sci., Rev. Macromol. Chem. Phys.* **1989**, *C29*, 201.

(12) Bruch, M. D.; Payne, W. G. *Macromolecules* **1986**, *19*, 2712.

(13) Beshah, K. *Macromolecules* **1992**, *25*, 5597.

(14) Dutta, K.; Mukherjee, M.; Brar, A. S. *J. Polym. Sci., Part A: Polym. Chem.* **1999**, *37*, 551.

(15) Wyzgoski, F. J.; Rinaldi, P. L.; McCord, E. F.; Stewart, M. A.; Marshall, D. R. *Macromolecules* **2004**, *37*, 846.

(16) Bodenhausen, G.; Ruben, D. J. *Chem. Phys. Lett.* **1980**, *69*, 185.

(17) Bax, A.; Summers, M. F. *J. Am. Chem. Soc.* **1983**, *108*, 2093.

(18) Lerner, L.; Bax, A. *J. Magn. Reson.* **1986**, *69*, 375.

(19) Davis, D. G. *J. Magn. Reson.* **1989**, *84*, 417.

(20) Wu, T. K.; Ovenall, D. W.; Hoehn, H. H. In *Applications of Polymer Spectroscopy*; Brame, E. G., Ed.; Academic: New York, 1978; pp 19−40.

(21) McCord, E. F.; Shaw, W. H., Jr.; Hutchinson, R. A. *Macromolecules* **1997**, *30*, 246.

(22) Newmark, R. A.; Battiste, J. L.; Koivula, M. N. *ACS Symp. Ser.* **2003**, *834*, 179.

(23) Roedel, M. J. *J. Am. Chem. Soc.* **1953**, *75*, 6110.

MA070327L